Computation of the lead-field matrix

Conference Paper · August 2023

CITATIONS
0

READS
569

3 authors, including:

Mohammad Orabe
Technische Universität Berlin
2 PUBLICATIONS **0** CITATIONS
SEE PROFILE

Zixuan Liu
Technische Universität Berlin
2 PUBLICATIONS **0** CITATIONS
SEE PROFILE

A Lead-Field Matrix for Neurolib

Zixuan Liu, Mohammad Orabe
zixuan.liu@campus.tu-berlin.de, orabe@campus.tu-berlin.de
Supervisor: Caglar Cakan
Neural Information Processing Group - Technische Universität Berlin

Abstract

The objective of our project is to construct a lead-field matrix corresponding to the Automated Anatomical Labeling 2 (AAL2) atlas and standard 1020 electroencephalography (EEG) electrode configuration, utilizing computational resources such as the MNE Python or the Matlab FieldTrip toolbox. Upon acquisition of the matrix, it will be integrated into the neurolib framework.

1 Introduction

1.1 Forward- and inverse modeling

The process of predicting the distribution of EEG potentials or magnetoencephalographic (MEG) fields given a known neural source is termed as forward modeling. Conversely, the process of deducing the unidentified neural sources from the observed EEG or MEG data is termed as inverse modeling.

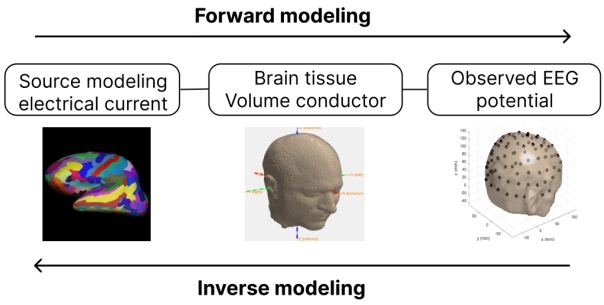

Figure 1: Illustration of forward and inverse modeling

1.2 Physiological source

The physiological source, referring to the tissue responsible for generating the electric current, is illustrated in Figure 1, which depicts neatly aligned neuron dendrites. The occurrence of action potentials at the synapses instigates a current flow along the dendritic tree, subsequently permeating through the entire brain tissues.

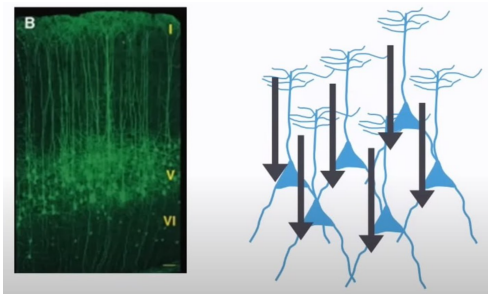

Figure 2: Image of dendrites and modeling

In principle, each dendritic tree can be represented using an equivalent current dipole model, a physical construct that describes a system with two poles, such as a positive and a negative charge. This dipole model offers a simplified depiction of neurons. However, due to limitations in resolution and computational power, it is impractical to model each neuron individually.

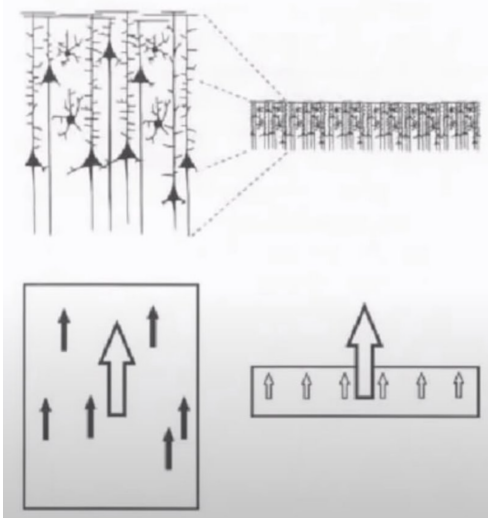

Figure 3: Source dipole model

Consequently, a specific region or segment can be selected, and the multitude of small equivalent

current dipoles within it is simplified into a single, larger equivalent current dipole, as illustrated in Figure 2. This approach is applicable to relatively large cortical patches, given that the recordings are obtained from a considerable distance.

1.3 Volume conductor

The volume conductor delineates the electrical characteristics of the tissue, the geometric model of the head, and the path of electric current flow. However, it does not specify the origin of the electric current. Numerous computational methodologies exist for volume conductors with realistic geometries, including Boundary Element Methods (BEM), Finite Element Methods (FEM), and Finite Difference Methods (FDM).

1.3.1 Boundary Element Method

The BEM in forward modeling assumes the head is composed of multiple homogeneous and isotropic compartments, each with uniform conductivity [1]. This simplification overlooks the fact that current flows easier along white matter tracts than across them. The model typically considers three tissue types: skin, skull, and brain, each with distinct electrical conductive properties. Sometimes, cerebrospinal fluid (CSF) is also included as a thin layer between the brain and the skull. The term ”brain” here encompasses all tissue within the skull, including white and gray matter, and is assumed to have homogeneous conductivity. The boundaries between these tissue types are described using triangles, which are flexible in describing complex, closed surfaces.

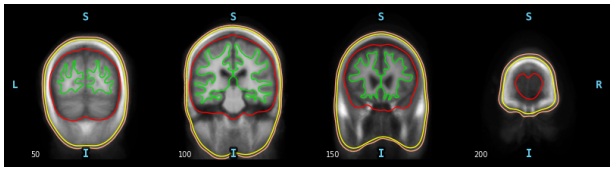

Figure 4: BEM for the template date ”fsaverage”

The BEM process begins with anatomical magnetic resonance imaging (MRI), which is segmented into different tissue types. The boundaries between these tissue types are then extracted and downsampled to a manageable number of triangles. Once the geometry is established and conductivities assigned, the model is computed independently of the source model, allowing for the results to be stored for future use. This computation is time-consuming but only needs to be performed once. If processed with sufficient detail, the BEM can include skull holes, but this is relatively uncommon due to the complexity of creating detailed anatomical models.

1.3.2 Finite Element Method

The FEM is another approach for volume conduction modeling in which the 3D volume is divided into small tetrahedral or volumetric elements.

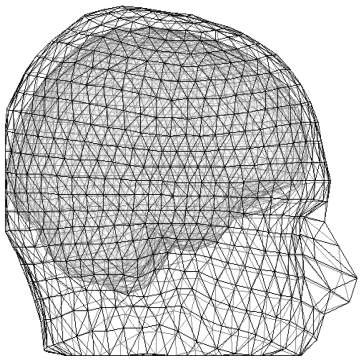

Figure 5: FEM for an exemplary head model

Unlike BEM which describes only surfaces, FEM encapsulates the entire volume, necessitating a larger number of elements[2]. Nevertheless, FEM allows for simplification by using larger volume elements in areas where less accuracy is needed, such as deep within the brain, and more elements where precision is crucial, like around the skull. Each tetrahedron in FEM can have its unique, potentially anisotropic, conductivity, making FEM the most accurate numerical method currently available for solving the forward problem. Despite its accuracy, FEM is computationally expensive and time-consuming, limiting its widespread use.

1.4 Coordinates and atlas

A prerequisite of forward modeling is that the geometrical description of the sensor positions, head model, and source model are expressed in the same coordinate system (e.g., CTF, MNI, Talairach) and with the same units (mm, cm, or m). There are different conventions for coordinate systems.

1.4.1 Talairach coordinates

Talairach coordinates [3], also known as Talairach space, constitute a three-dimensional coordinate system or ’atlas’ of the human brain, facilitating

the mapping of brain structures irrespective of individual variations in brain size and morphology.
The framework of the Talairach coordinate system involves positioning two reference points, the anterior commissure and posterior commissure, along a straight horizontal line [4]. With these two points lying on the midsagittal plane, the orientation of this plane as vertical entirely defines the coordinate system. The anterior commissure acts as the origin for measuring distances, with the y-axis pointing anterior and posterior to the commissures, the x-axis defining left and right, and the z-axis indicating the ventral-dorsal directions. Upon reorienting the brain to these axes, the six cortical outlines are delineated: anterior, posterior, left, right, inferior, and superior[5].

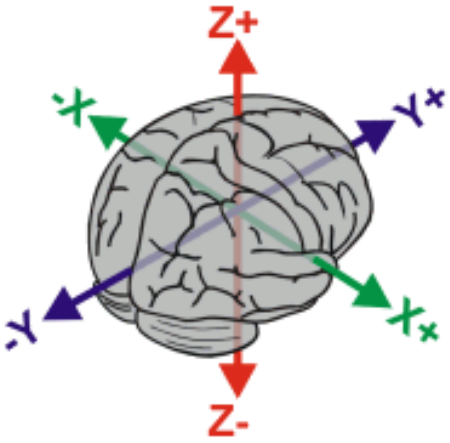

Figure 6: Example of x-,y-,z-axis of Talairach coordinate [6]

The standardization of these anatomical landmarks facilitates the spatial warping of individual brain images obtained through MRI, positron emission tomography (PET), and other imaging methods to this standard Talairach space, enabling inferences about tissue identity at specific locations by referring to the atlas.
In our project, the Matlab script was deployed in the context of the Talairach coordinate system.

1.4.2 Montreal Neurological Institute coordinate

Montreal Neurological Institute (MNI) coordinates are a system used for spatial normalization of brain images. Unlike the Talairach and Tournoux atlas, which is based on a single dissected brain, MNI coordinates were defined from the average of 305 MRI scans to create a standard brain template called MNI305 [7], this brain is considered more representative of the population than the Talairach brain.
However, differences exist between the MNI and Talairach brain templates, with the former being slightly larger and varying in spatial dimensions, particularly towards the brain's periphery. Converting MNI coordinates to Talairach coordinates is not straightforward due to these differences in brain shape and size.
Despite these disparities, Statistical Parametric Mapping (SPM) software uses MNI brain templates for spatial normalization, referring to the resulting coordinates as being in Talairach space [8], due to their shared coordinate systems.
The AAL2 atlas, which is employed in our project, operates within the framework of the MNI Coordinate System.

1.5 Objective

The objective of our project is to compute the leadfield matrix, a matrix that fundamentally characterizes the responsiveness of each EEG electrode sensor, to every potential neural source location within the brain. The employment of the leadfield matrix not only facilitates the computation of the forward solution but also provides a straightforward method for calculating inverse modeling.

2 Methodologies

2.1 Automated Anatomical Labeling 2

The AAL process involves an anatomical parcellation of the spatially normalized, high-resolution MRI provided by the MNI. The primary sulci of the MNI single-subject were delineated and used as landmarks for defining 45 anatomical volumes of interest (AVOI) in each hemisphere. This was achieved using dedicated software that allowed 3D tracking of the sulci course on the edited brain. Regions of interest were manually drawn every 2mm on the axial slices of the MNI single subject, and the 90 AVOI were reconstructed and labeled. This method proposes three procedures for the automated anatomical labeling of functional studies: labeling of an extremum defined by coordinates, percentage of voxels in each AVOI intersected by a sphere centered by coordinates, and percentage of voxels in each AVOI intersected by an activated cluster [9].
In the AAL2 atlases, each hemisphere of the brain is characterized by 60 distinct AVOI, culminating in a comprehensive total of 120 AVOI across both

hemispheres [10].

2.2 Lead-field matrix calculation

The lead-field matrix can be represented by the following equation:

$$\overrightarrow{y}_{m\times 1} = L_{m\times n}\overrightarrow{x}_{n\times 1}$$

where:

$\overrightarrow{y}$: m simulated EEG electrodes signals

L : Lead-field matrix

$\overrightarrow{x}$: n simulated brain activities

The matrix multiplication format can be written as:

$$\begin{pmatrix} y_1 \\ y_2 \\ \vdots \\ y_m \end{pmatrix} = \begin{pmatrix} L_{11} & L_{12} & \dots & L_{1n} \\ L_{21} & L_{22} & \dots & L_{2n} \\ \vdots & \vdots & \ddots & \vdots \\ L_{m1} & L_{m2} & \dots & L_{mn} \end{pmatrix} \begin{pmatrix} x_1 \\ x_2 \\ \vdots \\ x_n \end{pmatrix}$$

In the brain model, the tissue responsible for generating brain activity is referred to as a voxel. At a physical level, this brain activity can be approximated as a dipole. Given the independence and linearity of the dipole electromagnetic field generated by each voxel, the adopted mathematical strategy involves sequential voxel activation. When a voxel is activated with an estimated dipole strength, it induces a current flow that, through forward modeling, results in simulated EEG signal data. Once the simulated dipole strength of a voxel and the corresponding simulated EEG data are obtained, the corresponding column of the lead-field matrix can be computed.

For instance for the first column:

$$\begin{pmatrix} y'_1 \\ y'_2 \\ \vdots \\ y'_m \end{pmatrix} = \begin{pmatrix} L_{11} & 0 & \dots & 0 \\ L_{21} & 0 & \dots & 0 \\ \vdots & \vdots & \ddots & \vdots \\ L_{m1} & 0 & \dots & 0 \end{pmatrix} \begin{pmatrix} x_1 \\ 0 \\ \vdots \\ 0 \end{pmatrix}$$

where:

$\overrightarrow{y}'$: EEG electrodes signals when only x_1 is activated

This process is repeated for every column of the matrix. The final lead-field matrix is then obtained by linear aggregation of these results, which mathematically, given $L_{\mathrm{m,i}}$ representing the i-th column of the lead-field matrix, can be represented as:

$$\sum_{i=0}^{n} L_{\mathrm{m,i}} = L_{\mathrm{m\times n}}$$

Upon completion of the forward solution computation utilizing the MNE Python, the derivation of the lead-field matrix can be achieved.

2.3 Workflow

In our project, we predominantly employ the MNE Python to compute the lead-field matrix for the template MRI dataset, denoted as "fsaverage". This computation is conducted within the context of a standard 1020 EEG configuration, with the AAL2 atlas functioning as the source space. Notably, the "fsaverage" dataset can be replaced with user-specific data as necessitated.

The processing pipeline is as follows:

Step 1. Construct BEM

Download and load the template MRI data, "fsaverage". This is facilitated by the integrated download code *fetch_fsaverage()* in MNE Python. Subsequently, the corresponding BEM is constructed by invoking the function *mne.make_bem_model()* with ico=4 and the default conductivity parameters (0.3, 0.006, 0.3) for the three layers of skin, skull, and brain. It should be noted that the BEM can also be directly loaded, as the "fsaverage" data download via MNE automatically includes the BEM.

Input: The template MRI data, "fsaverage".

Output: BEM for "fsaverage".

Step 2. Generate surface source model

The approach to establishing an AAL2 atlas source space involves computing the average dipole value of all dipoles within each annotation of the atlas. Consequently, the initial task is to generate the requisite surface source space. Although the "fsaverage" data comes with a pre-established surface source space, it can also be computed by running the function *mne.setup_source_space()*.

Input: The template MRI data, "fsaverage".

Output: Surface source model.

Step 3. Standard EEG coregistration

Prior to loading the standard EEG configuration, it is necessary to cleanse the channel names to facilitate the usage of a standard 1020 montage. The EEG electrode locations, which are already situated in the fsaverage's space (MNI space) for standard 1020 configuration, then can be read and set by implementing the function *mne.channels.make_standard_montage()* with the parameter *"standard_1020"*. The coregistration can be visualized by employing the function *plot_EEG_montage*.

Input: The template MRI data, ”fsaverage”.
Output: Standard 1020 EEG montage.

Step 4. General forward solution calculation
The comprehensive forward solution, encompassing the surface source model and the standard 1020 EEG configuration, can be computed by employing the function *mne.make_forward_solution()* with the default parameter setting. Nevertheless, the parameter *n_jobs* can be adjusted contingent on the specifications of the hardware device.
Input: BEM for ”fsaverage”, surface source model, and standard 1020 EEG montage.
Output: General forward solution.

Step 5. Downsampling
Downsampling constitutes the parcellation and grouping of the dipoles of the surface source model into the AAL2 atlas annotations, this is followed by the computation of the mean dipole value for all dipoles encapsulated within each atlas annotation, resulting in a single dipole emblematic of one atlas annotation.
The AAL2 nii file contains the coordinate information for each annotation, necessitating loading for the calculation of each atlas annotation's average dipole value, However, the coordinate information embedded within the nii file is conserved in MNI space, so the initial step involves an affine transformation to coregistrate the head coordinates into MNI space. The ”fsaverage” template data already contains the requisite transformation file, denoted as *”fsaverage-trans.fif”*.
Subsequent to the aforementioned transformation, it becomes essential to also coregistrate the surface source dipole coordinates, extractable from the general forward solution, into the MNI space. This is achievable through the application of the *mne.head_to_mni()* function, utilizing the previously mentioned transformation file.
With the dipole coordinates appropriately transformed, it is now feasible to proceed with the computation of the mean dipole value for all dipoles contained within each atlas annotation.
Incorporating the EEG data present in the general forward solution, the execution of the computation of the lead-field matrix can be conducted.
Input: General forward solution, AAL2 nii file, affine transformation.
Output: Lead-field matrix.

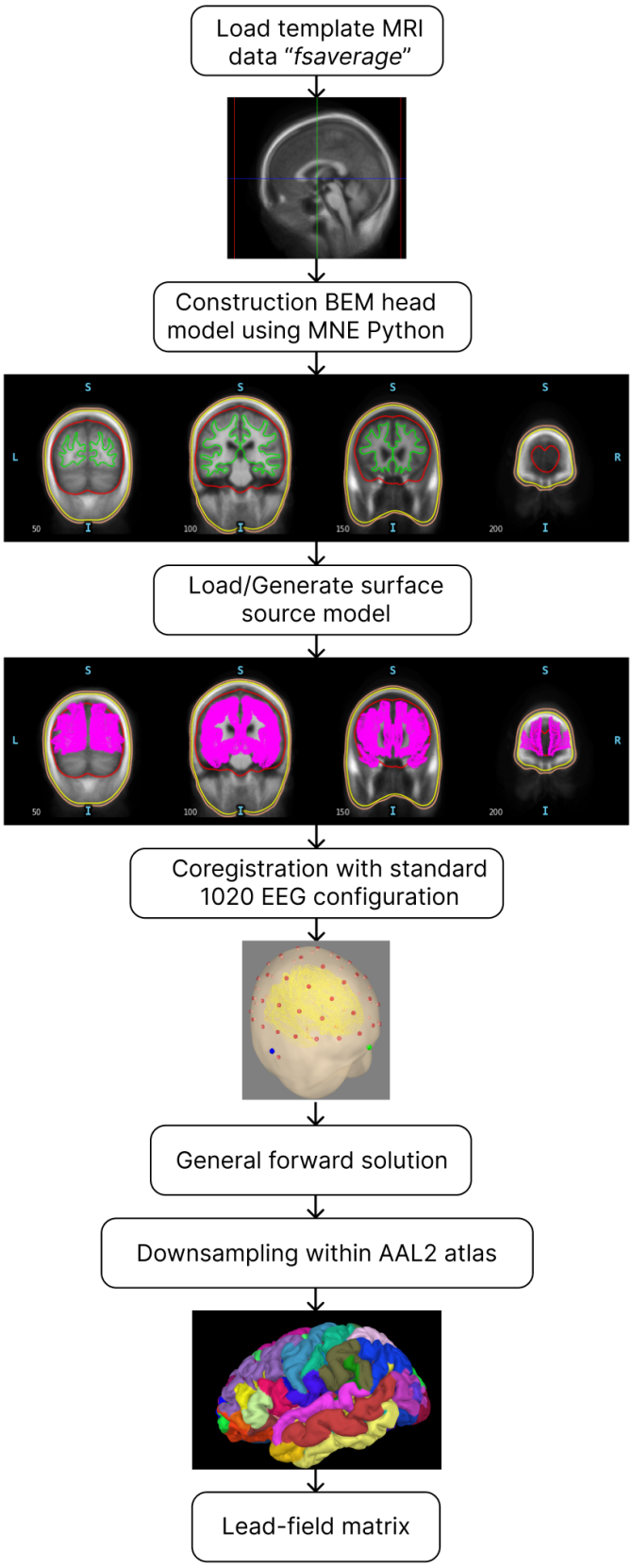

3 Results

3.1 MNE Python

Within the framework of the source model AAL2 Atlas, the lead-field matrix is computed utilizing the standard 1020 EEG configuration applied to the "fsaverage" template data, with the BEM serving for the construction of the head model. When the analysis is restricted to the cortical regions, excluding the subcortical areas, a matrix with dimensions corresponding to 64 sensors across 80 dipoles is successfully generated. However, the inclusion of subcortical regions results in a matrix with dimensions of 64 by 94, deviating from the expected 64 by 120. The potential causes of this discrepancy will be addressed in the discussion section.

The regions that are omitted are not uniformly distributed. For instance, within the region index range of 99-112, which corresponds to the cerebellum, most regions are absent, with the exception of indices 102 (*"Cerebellum 4 5 R"*) and 104 (*"Cerebellum 6 R"*). Furthermore, subcortical areas such as the Pallidum and Vermis are entirely missed.

3.2 Matlab

In the Matlab version, an attempt was made to calculate the lead-field matrix of the FEM using the Fieldtrip toolbox. However, due to time and resource constraints, progress was limited to the acquisition of the general forward solution with the source grid. The further downsampling process is still unfinished.

3.3 Open source codes

The Python code for computing the lead-field matrix example is accessible for further analysis at the following URL: https://github.com/neurolib-dev/neurolib/tree/master/examples.

4 Discussion

4.1 FEM in MNE

In the existing configuration of the MNE Python framework, there is a notable absence of support for FEM construction when developing head models. It is hypothesized that the implementation of FEM could potentially enhance the accuracy of forward modeling and the precision of the lead-field matrix. However, it should be noted that the development of a FEM-based head model is anticipated to necessitate a considerable augmentation in computational resources and an extended computational duration.

4.2 Missed subcortical regions

As noted in the results section, certain regions are absent in the computed lead-field matrix. A plausible explanation for this omission could be the absence of source dipoles in these regions within the constructed surface source model, particularly in subcortical components such as the cerebellum, thalamus, basal ganglia, amygdala, and hippocampus. Consequently, these regions are excluded during the downsampling process.

It is also worth noting that the creation of the surface source space, particularly when applying diverse "spacing" parameters within the *mne.setup_source_space()* function, leads to different regions being omitted. This indicates a significant variability in the model outcomes depending on the utilized parameters.

5 Conclusion

Our project successfully demonstrated the construction of a lead-field matrix for the AAL2 atlas in cortical areas with the standard 1020 EEG electrode configuration. This was accomplished within the MNE Python framework, leveraging the "fsaverage" template MRI dataset. The resulting lead-field matrix, an essential tool that characterizes the responsiveness of each sensor to all possible neural source locations within the brain, is pivotal for calculating both forward and inverse solutions.

The methodology, although productive, unveiled some challenges associated with the current computational procedures. Particularly, we noted an exclusion of certain brain regions, primarily subcortical components, in the resulting lead-field matrix. This was likely due to the lack of source dipoles in these regions within the developed surface source model. Additionally, varying "spacing" parameters in the surface source space generation resulted in disparate omitted regions.

In the absence of support for FEM construction within the MNE Python framework, the project used the BEM for head modeling. While the BEM is a robust and common method, the application of FEM could potentially provide a more accurate lead-field matrix, although with increased compu-

tational demands and time requirements.

Acknowledgments

We are profoundly grateful to Caglar Cakan from the Neural Information Processing Group at the Technische Universität Berlin for his guidance and support throughout the course of this project. His constructive feedback and direction have been instrumental in the successful completion of this work.
We would also like to express our deepest appreciation to Dr. Nikola Jajcay and Martin Krück from the Bernstein Center for Computational Neuroscience (BCCN) for their invaluable contributions to the solution of the downsampling process. Their expertise and insights have significantly enriched this research.

References

[1] Zeynep Akalin-Acar and Nevzat G Gençer. An advanced boundary element method (bem) implementation for the forward problem of electromagnetic source imaging. *Physics in medicine & biology*, 49(21):5011, 2004.

[2] Johannes Vorwerk, Anne Hanrath, Carsten H Wolters, and Lars Grasedyck. The multipole approach for eeg forward modeling using the finite element method. *NeuroImage*, 201:116039, 2019.

[3] Jean Talairach and G Szikla. Application of stereotactic concepts to the surgery of epilepsy. In *Advances in Stereotactic and Functional Neurosurgery 4: Proceedings of the 4 th Meeting of the European Society for Stereotactic and Functional Neurosurgery, Paris 1979*, pages 35–54. Springer, 1980.

[4] Yang MIAR, Jiang Guang-Zhong, et al. Medical imaging and augmented reality: Second international workshop, miar 2004, beijing, china, august 19-20, 2004: proceedings. *(No Title)*, 2004.

[5] Klaus D Toennies. *Guide to medical image analysis*. Springer, 2017.

[6] Jack L Lancaster, Marty G Woldorff, Lawrence M Parsons, Mario Liotti, Catarina S Freitas, Lacy Rainey, Peter V Kochunov, Dan Nickerson, Shawn A Mikiten, and Peter T Fox. Automated talairach atlas labels for functional brain mapping. *Human brain mapping*, 10(3): 120–131, 2000.

[7] Alan C Evans, D Louis Collins, SR Mills, Edward D Brown, Ryan L Kelly, and Terry M Peters. 3d statistical neuroanatomical models from 305 mri volumes. In *1993 IEEE conference record nuclear science symposium and medical imaging conference*, pages 1813–1817. IEEE, 1993.

[8] John Ashburner, Gareth Barnes, Chun-Chuan Chen, Jean Daunizeau, Guillaume Flandin, Karl Friston, Stefan Kiebel, James Kilner, Vladimir Litvak, Rosalyn Moran, et al. Spm12 manual. *Wellcome Trust Centre for Neuroimaging, London, UK*, 2464(4), 2014.

[9] Nathalie Tzourio-Mazoyer, Brigitte Landeau, Dimitri Papathanassiou, Fabrice Crivello, Octave Etard, Nicolas Delcroix, Bernard Mazoyer, and Marc Joliot. Automated anatomical labeling of activations in spm using a macroscopic anatomical parcellation of the mni mri single-subject brain. *Neuroimage*, 15(1):273–289, 2002.

[10] Edmund T Rolls, Marc Joliot, and Nathalie Tzourio-Mazoyer. Implementation of a new parcellation of the orbitofrontal cortex in the automated anatomical labeling atlas. *Neuroimage*, 122:1–5, 2015.